Rapid Exchange of Fluoroethylamine via the Rhesus Complex in Human Erythrocytes: ^{19}F NMR Magnetization Transfer Analysis Showing Competition by Ammonia and Ammonia Analogues†

David Szekely, Bogdan E. Chapman, William A. Bubb, and Philip W. Kuchel*

School of Molecular and Microbial Biosciences, University of Sydney, NSW 2006, Australia

Received March 14, 2006; Revised Manuscript Received June 1, 2006

ABSTRACT: A remarkable recent discovery in red blood cell function is that the Rhesus antigen complex that for so long was considered to be simply a means of cell recognition is also the ammonia transporter. It catalyzes transmembrane exchange of ammonia on the subsecond time scale, and yet because of a lack of rapid-exchange methodology its kinetics had not been characterized. The flux of ammonia varies appreciably in diverse clinical states, and a convenient method for its characterization would be of basic and of clinical diagnostic value. Fluoroethylamine is water-soluble and when added to a suspension of human red blood cells (RBCs) displays the experimentally useful property of giving separate ^{19}F NMR spectral peaks for the populations inside and outside the cells. By using two-site, one-dimensional magnetization exchange spectroscopy (1D-EXSY), the transmembrane exchange of fluoroethylamine was measured; it was found to occur on the subsecond time scale with an apparent first-order rate constant for efflux, under the equilibrium exchange conditions, of 3.4 s^{-1}. The method was used to characterize the concentration, temperature, and pH dependence of the exchange rate constant. We determined the extent of competitive inhibition exhibited by ammonia and two molecules that contain an amine group (ethylamine and methylamine). Inhibition of the exchange by incubating the suspension with anti-RhAG antibody, and no inhibition by anti-RhD antibody, suggested specificity of exchange via the RhAG protein of the Rh complex.

It was recently reported (*1*) that transmembrane exchange of ammonia in human red blood cells (RBCs)[1] occurs via channels belonging to the Amt/MEP/Rh superfamily. The focus of the present work was the membrane-transport function of the Rh family of proteins, three of which project from the surface of human RBCs: RhD (Rhesus protein expressing D antigen), RhCE (Rhesus protein expressing C or c antigens together with E or e antigens), and RhAG (Rhesus-associated glycoprotein), all of which contain 12 membrane-spanning domains. The Rh proteins have ∼20% homology with the methylamine permease (MEP) transporters and ammonia transporters (Amt) in yeast, bacteria, and simple plants (*2*). RhD protein is of great clinical importance as antibodies generated in vivo against it can cause major complications in pregnancy in which a fetus is RhD positive but the mother is RhD negative (but has developed anti-RhD antibodies in a previous pregnancy with an RhD positive fetus), resulting in hemolytic attack on the fetus (*3*, *4*).

The current structural model of the D antigens posits 37 epitopes disposed along the whole length of the protein, and since most of them are conformationally dependent, their exposure to antibodies will be influenced by other proteins, as well as lipids in the RBC membrane (*5*). Anti-D antibody binds to the D antigen (*6*), but accurate determination of the contact points between the two proteins awaits crystallographic analysis (*7*). In most D-negative populations, there is a deletion of the gene encoding the RhD protein (*7*).

The 170 kDa complex of the Rh proteins is seen to be a tetramer by density gradient ultracentrifugation, with two RhAG molecules and two RhCE or RhD protein molecules stabilized in the complex by associations between their respective N- and C-terminal domains (*8*−*10*). While the mechanism of transport and association of the three Rh proteins is not fully understood, the trimeric structure of AmtB presented by Khademi et al. (*1*) provides a concise explanation for how these proteins form the Rh complex in RBCs. The direct observation of the function of the transporter without added reagents as it operates on the subsecond time scale has hitherto not been possible. Assay of the transport activity has been routinely measured with the substrate analogue [^{14}C]methylamine that entails destructive analysis of the cell contents.

We discovered that an organic amine, 2-fluoroethylamine (FE), which is readily detectable by ^{19}F nuclear magnetic resonance (NMR) spectroscopy, has a characteristic that enables measurement of its rapid transmembrane exchange. The exchange is measured under conditions whereby the

† This work was funded by a Discovery grant from the Australian Research Council to P.W.K.

* To whom correspondence should be addressed. Phone: +61 2 9351 3709. Fax: +61 2 9351 4726. E-mail: p.kuchel@mmb.usyd.edu.au.

[1] Abbreviations: 1D-EXSY, one-dimensional exchange spectroscopy; 3FG, 3′-fluoro-3-deoxyglucose; Amt, ammonium transporters; EA, ethylamine; FE, fluoroethylamine; MA, methylamine; MEP, methyl permease; NMR, nuclear magnetic resonance; RBC, red blood cell; Rh, Rhesus; RhAG, Rhesus-associated glycoprotein; RhCE, Rhesus CE protein; RhD, Rhesus D protein.

10.1021/bi060505n CCC: $33.50
Published on Web 07/07/2006

solute is in electrochemical equilibrium across the membrane of the cell; the situation is called equilibrium exchange, and the NMR experiment to measure the transport is akin to adding a radioactive tracer to a solute-transport system that is already in electrochemical equilibrium.

When viewed along its C−C bond, FE has a cross section similar to that of ammonia so we postulated that its transport into RBCs would be mediated by the same protein(s) as is ammonia. We investigated the inhibition of FE transport by ammonia, and two small amines (methylamine and ethylamine), and by anti-Rh antibodies. The results led us to the conclusion that FE is an experimentally valuable analogue of ammonia, and the subsecond kinetics of the Rh membrane-transport complex could be studied under diverse conditions using the powerful NMR method of magnetization transfer. This can be done without the use of NMR shift reagents to give separate signals from inside and outside the cells, thus readily leading to a better understanding of the mechanism of operation of the Rh proteins.

MATERIALS AND METHODS

Solution Preparation. Solutions used to prepare RBCs were filtered three times through a 0.45 μm cellulose−nitrate membrane (Millipore, MA) in order to remove particulate matter (potentially paramagnetic or infective) and stored at 4 °C.

pH was measured and adjusted to a precision of ±0.05 pH units using a digital pH meter (model 1852MV; TPS, Brisbane, QLD) which was calibrated using pH 4.00, 7.00, and 10.00 standards (Merck, Kilsyth, VIC).

Osmolalities were measured using a Vapro vapor pressure osmometer, model 5520 (Wescor, Logan, UT), which was calibrated using a 290 mOsmol kg^{-1} standard (Wescor). Unless otherwise stated, all solutions used to wash and incubate RBCs were adjusted to 290 ± 10 mOsmol kg^{-1} with NaCl to ensure the normal volume and the shape of cells.

Preparation of RBCs. Freshly drawn venous blood was obtained by venipuncture from the cubital fossa of healthy donors; it was anticoagulated with heparin [15 units (mL of whole blood)$^{-1}$] and centrifuged for 10 min at 3000*g* at ∼4 °C in a swing-out rotor. The supernatant plasma and buffy coat containing the platelets and white blood cells were aspirated and discarded. The RBCs were resuspended in ∼4 volumes of isotonic saline (0.9% w/v NaCl) at 4 °C and centrifugally washed a further three times. Before the final wash, the cell suspension was gently bubbled with CO for ∼5 min to convert the hemoglobin to the stable carbonmonoxy form that is diamagnetic (*11*). The final hematocrit (Ht) was ∼0.9. Hematocrits were measured in duplicate using a microhematocrit centrifuge (Clements, North Ryde, NSW); a microhematocrit reader (Hawksley and Sons Ltd., Poole, U.K.) yielded a precision of ±0.5% in this estimate. For NMR experiments RBC suspensions (350 μL, final Ht ∼0.63) were incubated with FE at 37 °C in a 5 mm 507-PP NMR tube (Wilmad, Buena, NJ).

NMR Spectroscopy. All NMR spectra were acquired on a Bruker DRX-400 spectrometer (Bruker, Karlsruhe, Germany), equipped with a 9.4 T wide-bore vertical magnet (Oxford Instruments, Oxford, U.K.), at a radio frequency (rf) of 376.43 MHz for ^{19}F and 400.13 MHz for ^{1}H, using a 5 mm dual ^{1}H/^{19}F probe head (Bruker), where the ^{1}H channel was used for proton decoupling of the spectra.

Spectra for magnetization transfer studies were obtained by averaging eight transients into 4K data points using a spectral width of 2 kHz. A relaxation delay of 11 s (5 T_1) was used for FE exchange studies. In experiments where 3-fluoro-3-deoxyglucose (3FG) was added to the cell suspension, a relaxation delay of 5 s was used for 3FG exchange measurements. Fully relaxed spectra were recorded with a $\pi/2$−acquire pulse sequence. Magnetization exchange spectra were obtained with the 1D-EXSY pulse sequence (*12*): $\pi/2$−evolution−$\pi/2$−mixing time−$\pi/2$−acquisition.

The transmitter frequency was placed at either the intra- or extracellular peak frequency, and spectra were obtained at four evolution times, 3 μs (nominal zero), $^1/_8$, $^1/_4$, and $^1/_2$ $\delta\nu$, where $\delta\nu$ is the chemical shift difference, in hertz, between the intra- and extracellular peaks. For each evolution time, two spectra with mixing times of 3 μs (nominal zero) and 0.4 s were obtained. The transmitter frequency was then placed at the frequency of the other peak, and the experiment was repeated. Combined with the fully relaxed spectrum, this resulted in 17 spectra. The peak integrals from these spectra were then used in an "overdetermined" 1D-EXSY analysis, as described previously (*12*), to solve the equation:

$$\mathbf{M}(t) = e^{-Et}\mathbf{M}(0) \quad (1)$$

Spectra obtained with a mixing time of zero were used to construct the matrix **M**(0), the initial values of the magnetization, and those obtained with a mixing time of 0.4 s were used to construct the matrix **M**(t), the net magnetization after exchange. T_1 denotes the longitudinal nuclear magnetic relaxation time. The matrix **E** is the exchange matrix, consisting of T_1 relaxation and exchange rate constants. All experiments were recorded at 37 °C except those that were used to acquire an Arrhenius plot, in which the temperature was varied from 283 to 313 K. A line broadening factor of 3 Hz and zero filling to 8K were applied before Fourier transformation of each free induction decay.

The spectra were processed using XWINNMR, Version 3.5 (Bruker); they were phased and baseline-corrected prior to quantification of peaks. Clearly resolved peaks were integrated and overlapping ones deconvoluted, with a mixture of Lorentzian and Gaussian line shapes, using the relevant routines in XWINNMR.

For the study of pH dependence of FE transport rates, washed RBCs were suspended in PBS containing 10% D_2O, 20 mM Na_2HPO_4/NaH_2PO_4, and 8 mM FE. The cell suspension was titrated to pH values ranging from 6 to 9. The Ht was adjusted to 0.6, and 1D-EXSY spectra were then acquired.

For the studies of the effect of anti-RhD and anti-RhAG antibodies on the transport rate of FE, human polyclonal anti-RhD antibodies were obtained from the Royal Prince Alfred Hospital Blood Bank, Sydney, NSW, and monoclonal mouse anti-RhAG antibodies were obtained from the Sanquin Blood Supply Foundation (Amsterdam, The Netherlands). As the antibody solutions contained preservatives and were in hypertonic media, they were diluted 5-fold and made isotonic prior to use. Freshly drawn venous blood from an RhD positive donor was incubated with antibodies at concentrations varying between 0.5 and 3 times the concentration of the Rh antigen calculated for that suspension of RBCs. The suspension was centrifuged at 3000*g* for 8 min and resus-

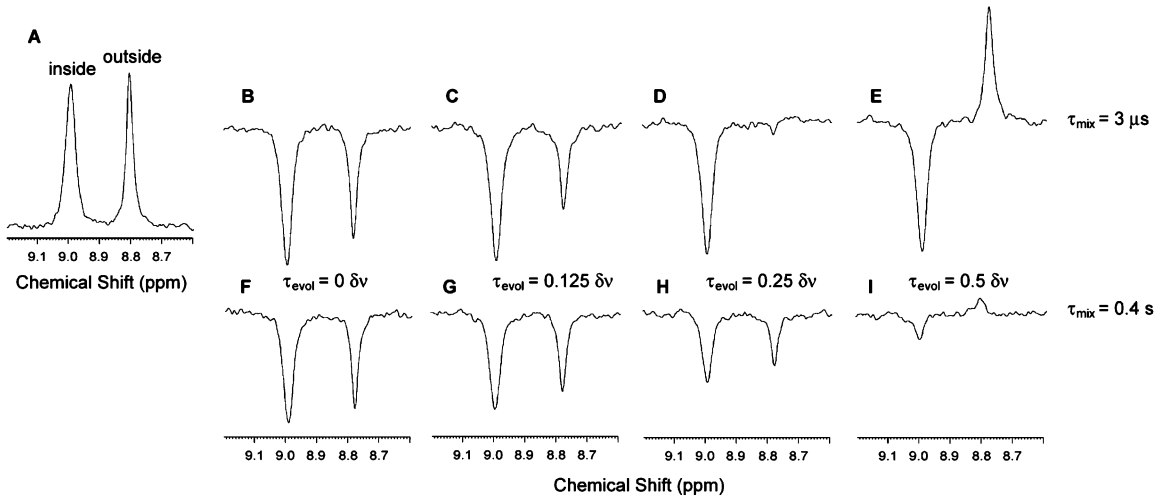

FIGURE 1: ^{19}F,^{1}H-decoupled NMR 1D-EXSY spectra of FE (3.2 mM) in a RBC suspension (Ht 0.68) at 37 °C. (A) is the fully relaxed equilibrium spectrum showing the high-frequency intracellular and low-frequency extracellular peaks. The upper spectra (B−E) were acquired with the 1D-EXSY pulse sequence, and the intracellular peak was inverted by setting the transmitter frequency to its chemical shift and with 3 μs (nominal zero) mixing time (τ_{mix}) and evolution times (τ_{evol}) of 3 μs, $^1/_8$ $\delta\nu$, $^1/_4$ $\delta\nu$, $^1/_2$ $\delta\nu$ s, where $\delta\nu$ is the peak separation in hertz. The lower spectra (F−I) were acquired with the same parameters except the mixing time was 0.4 s. A further four pairs of spectra (not shown), with the extracellular peak inverted, were acquired with the same parameters, thus giving the 17 spectra used in the 1D-EXSY analysis.

pended in saline to an Ht of 0.6 before the addition of 8.0 mM FE and subsequent acquisition of 1D-EXSY spectra. The extent of anti-RhD binding to the suspension was measured via incubation with CSL Abtectcell III 3% and anti-RhAG binding measured with a FACSCalibur flow cytometer (BD BioSciences, San Jose, CA) at 488 nm after incubating cells with equimolar fluorescent anti-mouse antibody. A control was used whereby RBCs with no anti-RhAG were incubated with mouse anti-DNP-9 (DNP-9 is absent in RBCs) at the concentrations used for the anti-RhAG experiments.

Data Analysis. 1D-EXSY spectra were analyzed using the method of Bulliman et al. (*12*) in a program that was converted to *Mathematica* (*13*). Regression analyses, both linear and nonlinear, were carried out with standard functions in *Mathematica*.

RESULTS

Exchange Kinetics. An initial ^{19}F NMR experiment showed that FE became equilibrated between the intra- and extracellular compartments of RBC suspensions in the time it took to obtain the first spectrum, ~2 min. Subsequently, it was found that a significant fraction of the population of spins in the high-energy state exchanged across the membrane within the longitudinal relaxation time; hence the transmembrane exchange rate was able to be determined with a 1D-EXSY (*12*) experiment (Figure 1).

Figure 1A shows the fully relaxed ^{19}F NMR spectrum of FE in a suspension of RBCs. The separation between the intracellular and extracellular FE resonances ($\delta\nu$) was 69 Hz, or 0.18 ppm. This value decreased slightly with increased FE concentration (2 Hz between 1.36 and 20.4 mM), decreased with increased temperature (10 Hz between 283 and 313 K), remained approximately constant with addition of other molecules (3FG, NH_3, MA, EA, etc.), and reached a maximum of 69 Hz at pH 7.4, decreased to a minimum of 53 Hz at pH 6.5, and became 46 Hz at pH 9 after inverting at pH 8.5. These values are consistent with other chemical shift differences found with fluorinated substances. Panels B−E of Figure 1 show the spectra from the 1D-EXSY experiment with the transmitter set to the frequency of the intracellular FE peak. The upper spectra (B−E) were acquired with a mixing time of 0 s and evolution times of 0, $^1/_8$, $^1/_4$, and $^1/_2$ $\delta\nu$ s; these peak intensities became the components of the matrix **M**(0) (*12*). The lower spectra in Figure 1 (F−I) were obtained with the same evolution times but with a mixing time of 0.4 s; these peak intensities became the components of the matrix **M**(t). The effect of magnetization transfer can be most readily seen in the pair of spectra in Figure 1E. The large positive intensity (initial magnetization) of the extracellular peak in the upper spectrum was reduced to a slightly negative value in the lower spectrum. This effect was due to inverted magnetization being transferred from the intracellular population to the extracellular population, in the mixing time, 0.4 s. The large extent of magnetization transfer heralded a statistically robust outcome for the kinetic analysis. Thus, 1D-EXSY analysis (*12*) yielded a rate constant for FE efflux at 3.4 mM (extracellular FE concentration) of 3.39 ± 0.02 s^{-1}. This was ~4-fold less than the rate constant of 12.8 ± 0.7 s^{-1} quoted for ammonia efflux from liposomes containing the Rh complex (*14*). The nominal stock concentration of FE of 10 mM that was added to the RBC suspensions, for most of the experiments, yielded an extracellular (electrochemical equilibrium) concentration of 3.4 mM and an intracellular concentration of 4.1 mM. This overall concentration was chosen because it was the optimal one, taking into account tradeoffs in reducing the experiment time, maximizing the signal-to-noise ratio of the data, and minimizing interference with the RBC suspension through factors such as osmotic pressure.

Membrane Potential. The relative peak intensities in Figure 1A were used in the Nernst equation to calculate the membrane potential ($\Delta\psi$) of the RBCs (*15*):

$$\Delta\psi = \frac{RT}{F}\ln\left(\frac{[\text{outside}]}{[\text{inside}]}\right) \qquad (2)$$

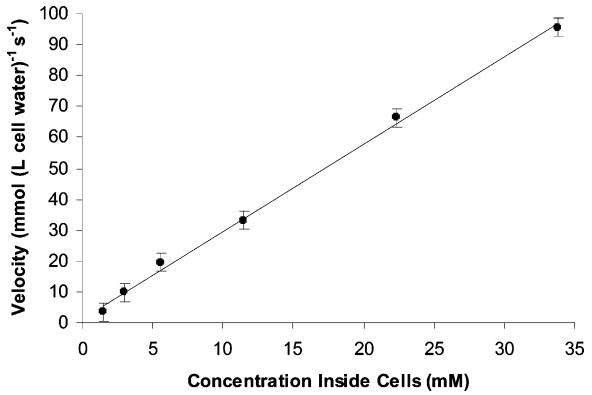

FIGURE 2: Transport rate of FE versus its concentration in RBC suspensions (Ht 0.64) at 37 °C. Each data point corresponds to the value obtained from a single 1D-EXSY experiment that also yielded an estimate of the standard deviation, shown in the corresponding error bar. The data were fitted by linear least-squares regression to give the line $y = 2.7437x + 1.7985$, yielding $R^2 = 0.9984$.

where R is the universal gas constant (8.314 J K^{-1} mol^{-1}), T is the absolute temperature in kelvin, F is Faraday's constant (96.5 $\times$ 10^3 C mol^{-1}), and [outside] and [inside] denote the concentrations of the monovalent cation in the corresponding compartments. Thus eq 2 yielded a membrane potential of -10.06 ± 0.05 mV, which is in excellent agreement with the value of ~ -10 mV that is normally reported (*16*).

Further 1D-EXSY experiments were undertaken to determine (1) at what concentration the exchange of FE became saturated, (2) the temperature dependence of the exchange rate and hence an estimation of the activation energy for the exchange, (3) the extent of competitive inhibition of exchange by added NH_4^+, and (4) whether inhibition would occur through binding of anti-Rhesus factor antibodies to the RBCs.

In studying the concentration dependence of the exchange rate, the final intracellular concentrations of FE ranged from 1.1 to 33.5 mM. Rate constants for the higher concentrations of FE could not be reliably obtained for isovolumic RBCs because the osmolality of the suspension exceeded 290 mOsmol L^{-1}. The results are given in Figure 2. A straight line fitted well to the data, indicating that the exchange was nonsaturable in the studied concentration range of FE. Therefore, values for the parameters V_{max} and K_m could not be independently determined.

Activation Energy. The dependence of the exchange rate of FE on temperatures ranging from 283 to 313 K was measured. To find the activation energy of the transport, an Arrhenius plot was constructed (Figure 3). Linear regression analysis of the unweighted data yielded an estimate of the activation energy of 62.1 $\pm$ 0.2 kJ mol^{-1}.

pH Dependence. The dependence of exchange of FE on pH was measured by titrating RBC suspensions to pH values ranging from 6 to 9. Rate constants were obtained only for the experiments with pH in the range 6−8 since the two peaks were not well resolved beyond pH 8 and the analysis could not be reliably applied; the peak overlap arose because the chemical shifts of both the intra- and extracellular peaks changed to higher frequencies, but the latter was to a larger extent.

The relationship between pH and transport rate constant for FE is shown in Figure 4. Both curves in Figure 4 show

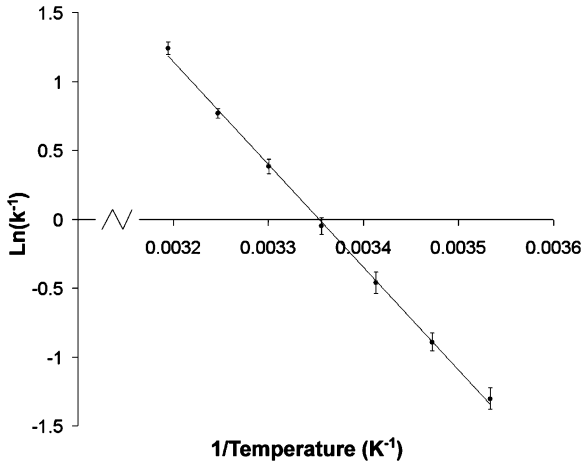

FIGURE 3: Arrhenius plot of the rate constant for FE exchange across the membranes of RBCs (Ht 0.6). Each of the seven data points corresponded to the result from an individual 1D-EXSY experiment. The gradient of the fitted line was −7468 K^{-1} that corresponds to an activation energy of 62.1 kJ mol^{-1}.

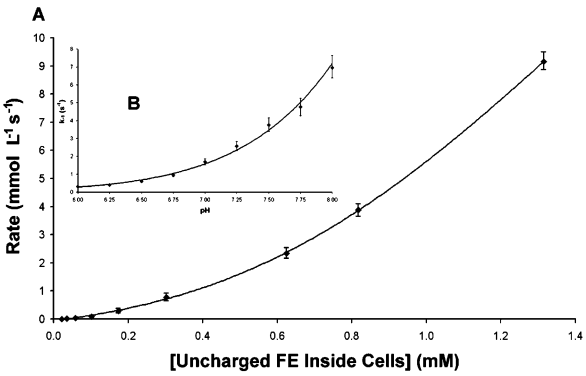

FIGURE 4: Dependence of the efflux rate constant of FE in RBCs on the intracellular pH. (A) Plot of the efflux velocity (concentration of intracellular uncharged FE $\times$ k_{-1}) versus the concentration of uncharged intracellular FE, calculated from the pK_a of FE (8.69), and the pH of the extracellular compartment (6.00, 6.25, 6.5, 6.75, 7, 7.25, 7.5, 7.75, and 8.00), respectively, at 37 °C. (B) Plot of k_{-1} versus pH. Each of the nine data points corresponded to the result from an individual 1D-EXSY experiment. The error bars denote the corrected values obtained from 1D-EXSY analysis (*12*). Intracellular pH was determined by taking into account the extracellular pH, hematocrit of the suspension, and the water-accessible space in the cells (α) (*15*). The empirical trendlines in (A) and (B) are to guide the eye.

exponential behavior, suggesting that membrane transport was mediated by a channel whose charge changed with pH. As the pH approached the pK_a of FE from below, an increasing fraction of FE would have been in the uncharged state, thus increasing the amount available for exchange via the transport channel. This would have led to an increase in the estimated rate constant. Since rate constants could not be obtained from the 1D-EXSY data for pH >8, the usual bell-shaped curve (*17*) was not evident.

Competition Studies. The effects of other amines, at concentrations between 8 and 80 mM, on the rate of FE exchange across the RBC membrane were studied. Ammonia/ammonium (NH_4^+), methylamine (MA), and ethylamine (EA) were added to suspensions of RBCs containing 8.0 mM FE and 8.0 mM 3FG, at 37 °C. The rate constants for exchange of the FE and 3FG (*18*) were determined from ^{19}F NMR 1D-EXSY experiments. These measurements were also made in the absence of 3FG; no effect was seen on the

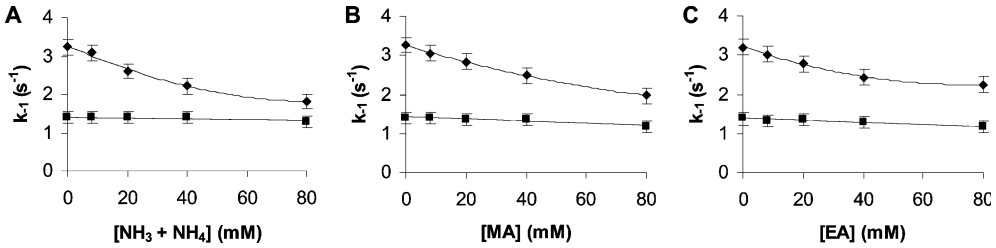

FIGURE 5: Apparent efflux rate constant for FE in suspensions of RBCs (Ht 0.6) obtained in the presence of other solutes: FE (8.0 mM) (◆) and 3FG (8.0 mM) (■) exchange rate constants estimated in the presence of 0, 8.0, 20.0, 40.0, and 80.0 mM (A) NH_3 + NH_4^+, (B) MA, and (C) EA. Each data point corresponds to the result from an individual 1D-EXSY experiment. The error bars denote the standard deviation obtained from 1D-EXSY analysis. The empirical trendlines are to guide the eye.

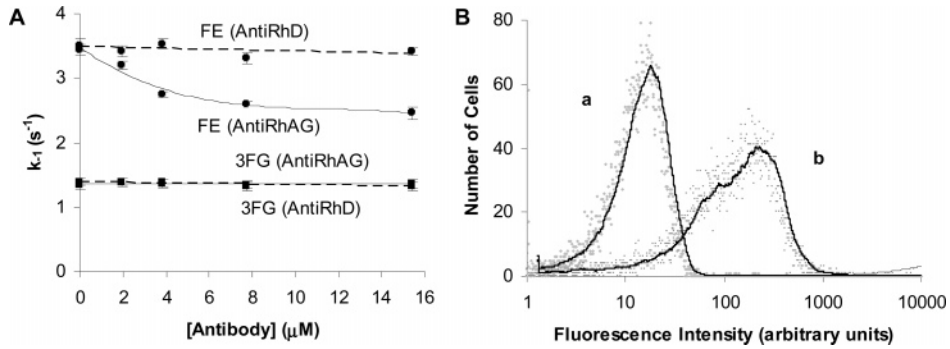

FIGURE 6: Dependence of the rate constant for FE efflux from human RBCs in the presence of anti-Rh antibodies. (A) Plot of FE (8.0 mM) (●) and 3FG (8.0 mM) (■) exchange rate constant values in RBCs (Ht 0.6) at 37 °C after incubation with 0, 1.93, 3.86, 7.72, and 15.44 μM anti-RhAG (solid line) and anti-RhD (dashed line). (B) Flow cytometry data from RBCs in (A) with (a) mouse anti-DNP-9 (negative control) and (b) mouse anti-RhAG (3.86 μM), both incubated with equimolar fluorescent anti-mouse antibody. Each data point in (A) corresponds to the result from an individual 1D-EXSY experiment. The error bars denote the error estimated from 1D-EXSY analysis (*12*). The empirical trendlines are to guide the eye.

exchange rate of FE in this situation (data not shown). The results are summarized in Figure 5.

There was marked reduction in the exchange rate of FE after the addition of ammonia and each of the amines, specifically 44%, 38%, and 30%, while the exchange rate of the 3FG was affected to a much lesser extent, with a reduction of 8%, 16%, and 15% in the presence of 80.0 mM NH_3 + NH_4^+, MA, and EA, respectively.

Antibody Effects. The inhibition of FE exchange in RBCs by mouse CD241 monoclonal antibody that was specific to a human RhAG antigen was also studied. Figure 6A shows a reduction of ~29% in the exchange rate constant estimated for FE and only a 5% decline in the rate constant for 3FG in the presence of anti-RhAG. Figure 6B shows that the RhAG antibody was bound to the RBCs in the suspension since there was significant separation in fluorescence intensities between the unbound anti-DNP-9−anti-mouse complex and bound anti-RhAG−anti-mouse complex. This is due to the unbound anti-DNP-9−anti-mouse complex producing a relatively less intense fluorescence signal than the RBC−anti-RhAG−anti-mouse complex. Had there been unbound anti-RhAG present in the suspension, then its mean fluorescence intensity would have decreased. A reduction in exchange rate constant for FE was not seen in the presence of bound anti-RhD.

DISCUSSION

Exchange Kinetics. The use of NMR spectroscopy to study rapid transmembrane exchange in cellular systems has the distinct advantage that the cells need not be separated from their surrounding medium to do the measurements, and experiments are performed under equilibrium exchange conditions (*19*−*21*). This gives information on biochemical composition, enzyme reaction rates, intracellular pH, and rates of membrane transport (*22*−*24*). In the present work, we exploited the utility of NMR to measure equilibrium exchange of FE in RBCs under numerous conditions including varying concentrations of FE, MA, EA, and NH_3/NH_4^+, temperatures between 283 and 313 K, pH to values between 6 and 8, and, finally, concentrations of anti-RhAG varying between 0.5- and 3-fold the concentration of the RhAG molecule in the suspension of cells.

Ripoche et al. (*25*) reported that the RhAG molecule mediates ammonia transport in human RBCs. Here, we extended these findings to a quantitative measurement of the kinetics of the process and show that the specific binding of the RhAG antibody to human RBCs results in a major reduction in the exchange rate of FE. The different chemical shifts (the "split-peak effect") for intra- and extracellular FE (*26*) allowed kinetic measurements in a convenient way and the simultaneous measurement of the membrane potential, both without the use of exogenous NMR shift reagents.

The "split peak" effect was first characterized by Kirk et al. (*26*); it was found that the amount of splitting of ^{31}P resonances for various phosphoryl compounds, including dimethyl methylphosphonate and the hypophosphite ion, depends almost solely on the hemoglobin concentration in the RBCs. The physical basis of the phenomenon is now known to be the diminution in the average extent of hydrogen bonding of the reporter atom (^{19}F), or oxygen bonded to it in the case of ^{31}P, to water inside the cells. This alteration arises because of the high intracellular protein concentration relative to outside the cells. There is little contribution to

the peak separation from magnetic susceptibility effects, contrary to an often held "belief" (*21*).

FE Permeability. The separation between the intra- and extracellular ^{19}F NMR peaks of FE, under normal conditions, was 69 Hz (Figure 1); given this good resolution of the peaks, inversion transfer analysis was made relatively simple. Panels E and I of Figure 1 show the extent of inversion transfer in RBCs with the inverted intracellular peak (Figure 1E) transferring a large proportion of its magnetization to the extracellular peak (Figure 1I) during the 0.4 s mixing time. The measured equilibrium exchange rate constant for FE was 3.4 s^{-1}, ~25% that of NH_3 (*14*). This smaller value is surmised to be due to its larger size and polarizability. It is difficult to predict (and virtually impossible through NMR means to determine) the effect that the zero-trans case would have on the rate constants since equilibrium between the two compartments occurs so rapidly. Determination of this effect relies on two key factors: (1) We must account for differences in osmotic pressure between internal and external compartments, since the relative concentrations of osmotic supports will be different in the zero-trans and the equilibrium cases. And (2), information about the pore protein must be available to interpret data obtained from such an experiment, such as the mechanism of transport, i.e., if there is a higher probability for the pore to exchange solute if substrate is bound to the internal face of the protein. Such data are currently not available for RhAG in human RBCs.

Figure 2 shows that, as seen with NH_3, the transport was not saturated up to concentrations of 35 mM, so it could be implied that the exchange occurs by simple diffusion via the phospholipid bilayer (*14*). However, we demonstrated that the efflux rate increased as the pH was raised. Since the amount of uncharged FE increases with increasing pH, this implies that it is the neutral form that is transported. The rate increase could also be attributed to a change in the protonation state of charged residues on the transporter protein, in which case a bell-shaped curve like that seen for many enzymes would be expected (*15*). However, in the present case, rate constant values were not obtained for suspensions with pH >8 since the intra- and extracellular peaks were not sufficiently well resolved to allow an accurate determination of their separate intensities (even using a spectral peak deconvolution method in XWINNMR).

The empirical curve fitted to the data in Figure 5 does not approach zero toward infinite ammonia, EA, or MA concentration. This appears to indicate that other, noncompetitive pathways are involved in the transport of FE. We have not, however, determined which other pathways are involved (if any), although it appears unlikely that another pathway is simple diffusion, since the partition coefficient of FE in a solution of monoleic acids is ~0 (unpublished data).

Thermodynamics. The activation energy, E_a, for the exchange of FE (62.1 kJ mol^{-1}) in human RBCs is similar to that for water permeability through pure lipid bilayers (46−60 kJ mol^{-1}) (*27*) but considerably higher than that for water in human RBCs (~25 kJ mol^{-1}) (*28*) and ~25% greater than that for ammonia (49.5 kJ mol^{-1}) (*14*). Taking a value for the enthalpy change required to break a hydrogen bond to be 10−20 kJ mol^{-1} (*29*), then the measured E_a is consistent with, or comparable to, the breaking of about four hydrogen bonds upon membrane transfer.

Studies on crystalline ammonia hydrates have shown that each of the four atoms of NH_3 can participate in hydrogen bonding (*30*). E_a values for the permeabilities of small molecules in liposomes correlate with the number of hydrogen bonds that can be formed with surrounding water and lipid atoms (*29*). Fluorine atoms are involved in hydrogen bonding, too, so the rates of deprotonation of the amine group and hydrogen bonding to the fluorine atom (*18*) could be significant contributors to the overall rate of the transport reaction.

In an equilibrium mixture of NH_3 and NH_4^+ in water the $[NH_3]$ is affected by the temperature dependence of the ionization constant (*30*). This corresponds to an increase in pK_a of 0.14 pH unit over the range 0−35 °C which leads to a reduction in available NH_3 at constant pH and a corresponding underestimate in E_a by ~5 kJ mol^{-1}. In RBC suspensions the intracellular pH falls as temperature increases because the isoelectric point of hemoglobin is inversely related to temperature (*31*). This effect would lead to a further reduction in NH_3 concentration. Thus, measuring the pH values at each temperature and correcting the apparent permeability estimates for the NH_3 concentration would have improved upon the interpretation of previous thermodynamic studies of ammonia influx.

Inhibition of FE Transport. As mentioned earlier, it has previously been reported that the channel protein RhAG conducts NH_3/NH_4^+ across the cell membrane (*25*). To confirm this, in the present work we attempted to specifically block ammonium ion transport. In the aforementioned study, *p*-(chloromercuri)benzenesulfonate (pCMBS) was used to inhibit the transport of NH_3 into RBCs (*25*). However, this reagent binds to sulfhydryl groups on many channel proteins, and it is known to affect water and urea transport but not anion transport (*32*). Ripoche et al. (*25*) found a reduction in NH_4^+ transport with pCMBS, and they posit two possible mechanisms of this effect: (1) NH_3 may bind to particular cysteine residues within the RhAG pore and noncompetitively inhibit transport, or (2) it could inhibit water transport and thus reduce flow of solutes into and out of the RBC. This would amplify the effect of an unstirred layer and reduce the rate at which NH_3 molecules would encounter the membrane as a precursor to moving across it through a transport protein. This compound therefore cannot be used to achieve specific inhibition of ammonia transport.

To study first whether FE was transported via the same pathway(s) as other amine-containing molecules, we noted that MA and EA and NH_3/NH_4^+ significantly reduced the exchange rate of FE, while 3FG transport, which is mediated by the GLUT-1 transporter (*17*), was only marginally affected. These results suggested specific, dose-dependent, competitive inhibition by cosubstrates of the transporter(s). Furthermore, under the conditions used, FE transport became saturated at high concentrations of inhibitor. Thus transport is via the same transmembrane protein(s).

We subsequently tested whether specific noncompetitive inhibition of the RhAG molecule could be attained with the anti-RhAG monoclonal antibody. In other systems, specific monoclonal antibodies can effectively inhibit transport of particular solutes across cell membranes (*33*−*35*). Specific antibodies have the distinct advantage over chemical reagents such as pCMBS in that, because a single epitope is bound by the antibody, no other protein is affected by its presence.

Figure 6 shows that FE exchange was significantly affected by anti-RhAG, and yet anti-RhD had no effect. Meanwhile, 3FG transport remained unaffected, within experimental error, in both instances. The details of the mechanism by which the anti-RhAG antibody inhibited the transmembrane exchange of FE have not been elucidated. There are a number of ways in which a molecule that binds to the extracellular face of a protein may inhibit exchange through it: (1) the relatively bulky antibody molecule could bind to a large area of the pore of the channel; (2) a conformational change could be induced on binding, causing a partial obstruction of the channel; and (3) there could be interference with key residues that are involved in the transport mechanism. For example, the mutation of the conserved Asp^{160} to Ala^{160} (found near the surface of the protein) in AmtB completely destroys transport of MA (*1*). This residue is surmised to be part of the amine "recruitment" site. It is possible that this aspartate residue was part of (or close to) the antibody binding site in our studies. And once bound, the residue could not participate optimally in the transport reaction, resulting in a reduction in FE exchange rate.

In conclusion, ^{19}F magnetization transfer NMR spectroscopy was used to study FE permeability in intact human RBCs under equilibrium exchange conditions on the sub-second time scale. FE transmembrane exchange in human RBCs was considered to be via RhAG. The apparent rate constant for the exchange of FE was higher than for water but significantly lower than that for ammonia. Unstirred layer effects may be rate determining for permeability, as pH and temperature increase, and this aspect of the behavior of the exchange requires further study. The activation energy, E_a, for FE permeability was 3 times greater than for water and ~50% greater than that for NH_3 transport; these effects are consistent with the different extents of hydrogen bonding evident with these two small molecules. The present ^{19}F NMR magnetization transfer technique should be applicable to other cellular systems for which amine transport and metabolism are of biomedical significance.

ACKNOWLEDGMENT

We thank Professor Noel Hush for bringing ref *1* to our attention and Professor Eugene Seneta for advice on the statistical analysis used in the 1D-EXSY experiments. We thank Professor Doug Joshua at the Department of Haematology, Royal Prince Alfred Hospital (RPAH), and Ms. Peggy Nelson at the RPAH blood bank for anti-D antibodies. Dr. Peter Stam is thanked for the anti-RhAG antibodies. Dr. Simon Easterbrook-Smith and Mr. Nathan Oates are thanked for help with the FACS analysis, and Mr. Bill Lowe is thanked for expert technical assistance.

REFERENCES

1. Khademi, S., O'Connell, J., III, Remis, J., Robles-Colmenares, Y., Miercke, L. J., and Stroud, R. M. (2004) Mechanism of ammonia transport by Amt/MEP/Rh: structure of AmtB at 1.35 Å, *Science 305*, 1587−1594.
2. Marini, A. M., Urrestarazu, A., Beauwens, R., and Andre, B. (1997) The Rh (rhesus) blood group polypeptides are related to NH_4^+ transporters, *Trends Biochem. Sci. 22*, 460−461.
3. Filbey, D., Berseus, O., and Carlberg, M. (1996) Occurrence of anti-D in RhD-positive mothers and the outcome of the newborns, *Acta Obstet. Gynecol. Scand. 75*, 585−587.
4. Bowman, J. M. (1998) RhD hemolytic disease of the newborn, *N. Engl. J. Med. 339*, 1775−1777.
5. Scott, M. (1996) Rh serology-coordinator's report, *Transfus. Clin. Biol. 3*, 333−337.
6. Kumpel, B. M. (2002) On the mechanism of tolerance to the Rh D antigen mediated by passive anti-D (Rh D prophylaxis), *Immunol. Lett. 82*, 67−73.
7. Avent, N. D., and Reid, M. E. (2000) The Rh blood group system: a review, *Blood 95*, 375−387.
8. Eyers, S. A., Ridgwell, K., Mawby, W. J., and Tanner, M. J. (1994) Topology and organization of human Rh (rhesus) blood group-related polypeptides, *J. Biol. Chem. 269*, 6417−6423.
9. Hartel-Schenk, S., and Agre, P. (1992) Mammalian red cell membrane Rh polypeptides are selectively palmitoylated subunits of a macromolecular complex, *J. Biol. Chem. 267*, 5569−5574.
10. Cartron, J. P. (1999) Rh blood group system and molecular basis of Rh-deficiency, *Bailliere's Best Pract. Res., Clin. Haematol. 12*, 655−689.
11. Cerdonio, M., Morante, S., Vitale, S., Dalvit, C., Russu, I. M., Ho, C., de Young, A., and Noble, R. W. (1983) Magnetic and spectral properties of carp carbonmonoxyhemoglobin. Competitive effects of chloride ions and inositol hexakisphosphate, *Eur. J. Biochem. 132*, 461−467.
12. Bulliman, B. T., Kuchel, P. W., and Chapman, B. E. (1989) "Overdetermined" one-dimensional NMR exchange analysis. A 1D counterpart of the 2D EXSY experiment, *J. Magn. Res. 82*, 131−138.
13. Wolfram, S. (2003) *The Mathematica Book*, 5th ed., Wolfram Media Inc., Champaign, IL.
14. Labotka, R. J., Lundberg, P., and Kuchel, P. W. (1995) Ammonia permeability of erythrocyte membrane studied by ^{14}N and ^{15}N saturation transfer NMR spectroscopy, *Am. J. Physiol. 268*, C686−C699.
15. Mulquiney, P. J., and Kuchel, P. W. (2003) *Modelling Metabolism with* Mathematica, CRC Press, Boca Raton, FL.
16. Lassen, U. V., Lew, V. L., Pape, L., and Simonsen, L. O. (1977) Transient increase in the K permeability of intact human and Amphiuma red cells induced by external Ca at alkaline pH, *J. Physiol. 266*, 72P−73P.
17. Kuchel, P. W., and Ralston, G. B. (1997) *Schaum's Outline of Theory and Problems of Biochemistry*, 2nd ed., McGraw-Hill, New York.
18. Potts, J. R., and Kuchel, P. W. (1992) Anomeric preference of fluoroglucose exchange across human red-cell membranes. ^{19}F-NMR studies, *Biochem. J. 266*, 925−928.
19. Benga, G., Matei, H., Borza, T., Porutiu, D., and Lupse, C. (1993) Comparative nuclear magnetic resonance studies of diffusional water permeability of red blood cells from different species. V-Rabbit *(Oryctolagus cuniculus)*, *Comp. Biochem. Physiol. B 106*, 281−285.
20. Decking, U. K., Alves, C., Spahr, R., and Schrader, J. (1994) 2-Fluoroadenosine uptake by erythrocytes and endothelial cells studied by ^{19}F-NMR *Am. J. Physiol. 266*, H1596−H1603.
21. Liu, D., Knauf, P. A., and Kennedy, S. D. (1996) Detection of Cl^- binding to band 3 by double-quantum-filtered ^{35}Cl nuclear magnetic resonance, *Biophys. J. 70*, 715−722.
22. Lundberg, P., Harmsen, E., Ho, C., and Vogel, H. J. (1990) Nuclear magnetic resonance studies of cellular metabolism, *Anal. Biochem. 191*, 193−222.
23. Kuchel, P. W. (1990) Spin-exchange NMR spectroscopy in studies of the kinetics of enzymes and membrane transport, *NMR Biomed. 3*, 102−119.
24. Kuchel, P. W., and Chapman, B. E. (1983) NMR spin exchange kinetics at equilibrium in membrane transport and enzyme systems, *J. Theor. Biol. 105*, 569−589.
25. Ripoche, P., Bertrand, O., Gane, P., Birkenmeier, C., Colin, Y., and Cartron, J. P. (2004) Human Rhesus-associated glycoprotein mediates facilitated transport of NH_3 into red blood cells, *Proc. Natl. Acad. Sci. U.S.A. 101*, 17222−17227.
26. Kirk, K., and Kuchel, P. W. (1988) Characterization of transmembrane chemical shift differences in the ^{31}P NMR spectra of various phosphoryl compounds added to erythrocyte suspensions, *Biochemistry 27*, 8795−8802.
27. Fettiplace, R., and Haydon, D. A. (1980) Water permeability of lipid membranes, *Physiol. Rev. 60*, 510−550.

28. Benga, G., Pop, V. I., Popescu, O., Hodarnau, A., Borza, V., and Presecan, E. (1987) Effects of temperature on water diffusion in human erythrocytes and ghosts-nuclear magnetic resonance studies, *Biochim. Biophys. Acta 905*, 339−348.
29. Cohen, B. E. (1975) The permeability of liposomes to nonelectrolytes. I. Activation energies for permeation, *J. Membr. Biol. 20*, 205−234.
30. Jolly, W. L. (1964) *The Inorganic Chemistry of Nitrogen*, pp 20−46, Benjamin, New York.
31. Reeves, R. B. (1976) Temperature-induced changes in blood acid−base status: Donnan rCl and red cell volume, *J. Appl. Physiol. 40*, 762−767.
32. Zhang, Z. H., and Solomon, A. K. (1992) Effect of pCMBS on anion transport in human red cell membranes, *Biochim. Biophys. Acta 1106*, 31−39.
33. Han, X., Chesney, R. W., Budreau, A. M., and Jones, D. P. (1996) Regulation of expression of taurine transport in two continuous renal epithelial cell lines and inhibition of taurine transporter by a site-directed antibody, *Adv. Exp. Med. Biol. 403*, 173−191.
34. Mol, J. A., Krenning, E. P., Docter, R., Rozing, J., and Hennemann, G. (1986) Inhibition of iodothyronine transport into rat liver cells by a monoclonal antibody, *J. Biol. Chem. 261*, 7640−7643.
35. Fejes-Toth, G., Naray-Fejes-Toth, A., Satlin, L. M., Mehrgut, F. M., and Schwartz, G. J. (1994) Inhibition of bicarbonate transport in peanut lectin-positive intercalated cells by a monoclonal antibody, *Am. J. Physiol. 266*, F901−F910.

BI060505N